AMERICAN SOCIETY FOR MICROBIOLOGY | Antimicrobial Agents and Chemotherapy®

ANTIVIRAL AGENTS

Thiostrepton Reactivates Latent HIV-1 through the p-TEFb and NF-κB Pathways Mediated by Heat Shock Response

Wen Peng,[a] Zhongsi Hong,[b] Xi Chen,[a] Hongbo Gao,[a] Zhuanglin Dai,[a] Jiacong Zhao,[a] Wen Liu,[c] Dan Li,[a,d] Kai Deng[a]

[a]Institute of Human Virology, Key Laboratory of Tropical Disease Control of Ministry of Education, Zhongshan School of Medicine, Sun Yat-sen University, Guangzhou, China

[b]Department of Infectious Diseases, Fifth Affiliated Hospital, Sun Yat-sen University, Zhuhai, China

[c]State Key Laboratory of Bioorganic and Natural Products Chemistry, Shanghai Institute of Organic Chemistry, Chinese Academy of Sciences, Shanghai, China

[d]Guangzhou Women and Children's Medical Center, Guangzhou, China

Wen Peng and Zhongsi Hong contributed equally to this work. Author order was determined by relative contribution in the study.

ABSTRACT Antiretroviral therapy (ART) suppresses HIV-1 replication but fails to cure the infection. The presence of an extremely stable viral latent reservoir, primarily in resting memory CD4$^+$ T cells, remains a major obstacle to viral eradication. The "shock and kill" strategy targets these latently infected cells and boosts immune recognition and clearance, and thus, it is a promising approach for an HIV-1 functional cure. Although some latency-reversing agents (LRAs) have been reported, no apparent clinical progress has been made, so it is still vital to seek novel and effective LRAs. Here, we report that thiostrepton (TSR), a proteasome inhibitor, reactivates latent HIV-1 effectively in cellular models and in primary CD4$^+$ T cells from ART-suppressed individuals *ex vivo*. TSR does not induce global T cell activation, severe cytotoxicity, or CD8$^+$ T cell dysfunction, making it a prospective LRA candidate. We also observed a significant synergistic effect of reactivation when TSR was combined with JQ1, prostratin, or bryostatin-1. Interestingly, six TSR analogues also show reactivation abilities that are similar to or more effective than that of TSR. We further verified that TSR upregulated expression of heat shock proteins (HSPs) in CD4$^+$ T cells, which subsequently activated positive transcriptional elongation factor b (p-TEFb) and NF-κB signals, leading to viral reactivation. In summary, we identify TSR as a novel LRA which could have important significance for applications to an HIV-1 functional cure in the future.

KEYWORDS HIV-1, latent reservoir, latency reversal agent, thiostrepton, heat shock protein

Despite the fact that antiretroviral therapy (ART) potently reduces plasma HIV-1 levels below the detection limit of clinical assays, the extremely stable viral latent reservoir in resting memory CD4$^+$ T cells remains the major barrier to HIV-1 eradication (1, 2). Latently infected cells contain a transcriptional silent form of the viral genome, which helps infected cells evade host immune surveillance. Viremia rapidly rebounds once treatment is discontinued; therefore, ART is not curative, and infected individuals must receive lifelong antiretroviral treatment (3–5). However, long-term ART administration leads to drug toxicity, drug resistance, and heavy financial burdens (6). Research exploring potential therapeutic strategies to target the HIV-1 latent reservoirs has accelerated significantly in recent years.

One potential approach to eliminate the latent HIV-1 reservoirs is "shock and kill" (7, 8), which involves pharmacologic reactivation of the latent viruses without causing global T cell activation and subsequent killing of the reactivated infected cells by inducing virus-specific immune responses (9). The previously reported latency-

Citation Peng W, Hong Z, Chen X, Gao H, Dai Z, Zhao J, Liu W, Li D, Deng K. 2020. Thiostrepton reactivates latent HIV-1 through the p-TEFb and NF-κB pathways mediated by heat shock response. Antimicrob Agents Chemother 64:e02328-19. https://doi.org/10.1128/AAC.02328-19.

Address correspondence to Dan Li, lidanphyllis@163.com, or Kai Deng, dengkai6@mail.sysu.edu.cn.

Received 22 November 2019
Returned for modification 10 December 2019
Accepted 17 February 2020
Accepted manuscript posted online 24 February 2020
Published 21 April 2020

reversing agents (LRAs) can be categorized into four classes based on their mechanisms: histone posttranslational modification modulators (histone deacetylase [HDAC] inhibitors), nonhistone chromatin modulators (p-TEFb activators), NF-κB stimulators (protein kinase C [PKC] activators), and miscellaneous compounds (6). These LRAs have been shown to induce robust viral reactivation in cellular models of HIV-1 latency, and some of them have been approved for clinical trials (10). However, there has not been any compelling evidence so far demonstrating that LRAs can reduce the HIV-1 latent reservoir effectively in various clinical trials (11). This could be due to the complexity of molecular mechanisms maintaining the latent reservoirs or to the suboptimal efficacy of LRAs. HDAC inhibitors such as vorinostat (SAHA) and others were also shown to impair the function of HIV-1-specific cytotoxic T lymphocytes (CTLs) and failed to reduce inducible HIV-1 reservoirs (12). Therefore, it is still vital and urgent that we search for novel compounds to reactivate latent HIV-1 with higher efficacy and lower immunogenic toxicity.

By using a primary $CD4^+$ T cell model of HIV-1 latency (13), we identified thiostrepton (TSR), which could reactive latent HIV-1 efficiently in cellular models and in primary $CD4^+$ T cells from ART-suppressed individuals *ex vivo*. TSR is a polythiazole peptide antibiotic isolated from cultures of *Streptomyces laurentii* (14). It was reported to exhibit strong activity against Gram-positive bacteria and malaria parasites, as well as anticancer activity in various cancer models (15–18). Moreover, TSR has also been shown to be a proteasome inhibitor (16, 19) and induces oxidative and proteotoxic stress by upregulating the expression of heat shock proteins (HSPs), oxidative stress, and endoplasmic reticulum (ER) stress, which induces apoptosis of cancer cells. Recently, proteasome inhibitors such as MG132, carfilzomib (CFZ), and bortezomib (BTZ) have been shown to possess HIV-1 latency reversal activities mediated by heat shock factor 1 (HSF1) and heat shock protein 90 (HSP90) (20). HSF1- and HSP-mediated activation of viral gene expression was reported recently (21–23), so we hypothesized that TSR may also act through heat shock response to induce HIV-1 transcription in latently infected cells, and our results suggest that this is indeed the case.

In summary, our study identified TSR as a novel LRA which can effectively induce HIV-1 transcription in latently infected cells and which has the potential to be further developed as a critical compound for the shock-and-kill strategy and HIV-1 functional cure.

RESULTS

TSR induces effective latent-HIV-1 reactivation *in vitro* and *ex vivo*. We used a primary $CD4^+$ T cell model of HIV-1 latency to screen for compounds that could potentially reverse latency (24). Latently infected cells were treated with compounds from the U.S. Drug Collection library for 48 h. Of the 1,280 compounds we screened, 3 exhibited effective reactivation abilities in our high-throughput platform (Fig. 1A). SAHA (25) and disulfiram (26) were previously reported as LRAs. TSR is a peptide antibiotic approved by the FDA for animal use (Fig. 1B) that has not been documented for its latency reversal capacity. TSR induced viral gene expression, as indicated by expression of green fluorescent protein (GFP), in a dose-dependent manner (Fig. 1C), and the optimal activity was at 1 μM for 48 h (Fig. 1C and D). Similar latency-reversing effects were also observed in J-Lat cells (Fig. 1E), a widely used model of HIV-1 latency (27). The optimal concentrations of TSR for the reactivation effect are 1 μM for J-Lat 10.6 and 2.5 μM for J-Lat A2 (Fig. 1E). To further confirm the ability of TSR to reactivate latent HIV-1, cell-associated viral RNA transcription (long terminal repeat [LTR], Gag, Vif, or Vpr) was measured by reverse transcription-quantitative PCR (RT-qPCR) in $CD4^+$ T cells from individuals with ART-suppressed HIV-1 infection following TSR or phorbol-12-myristate-13-acetate (PMA)–ionomycin treatment. TSR induced a 11.91-fold to 32.07-fold increase of HIV-1 transcription compared to the negative control (dimethyl sulfoxide [DMSO]) (Fig. 1F).

We further confirmed that TSR-induced apoptosis was minimal in healthy donor $CD4^+$ T cells, as measured by annexin V-propidium iodide (PI) double staining at a

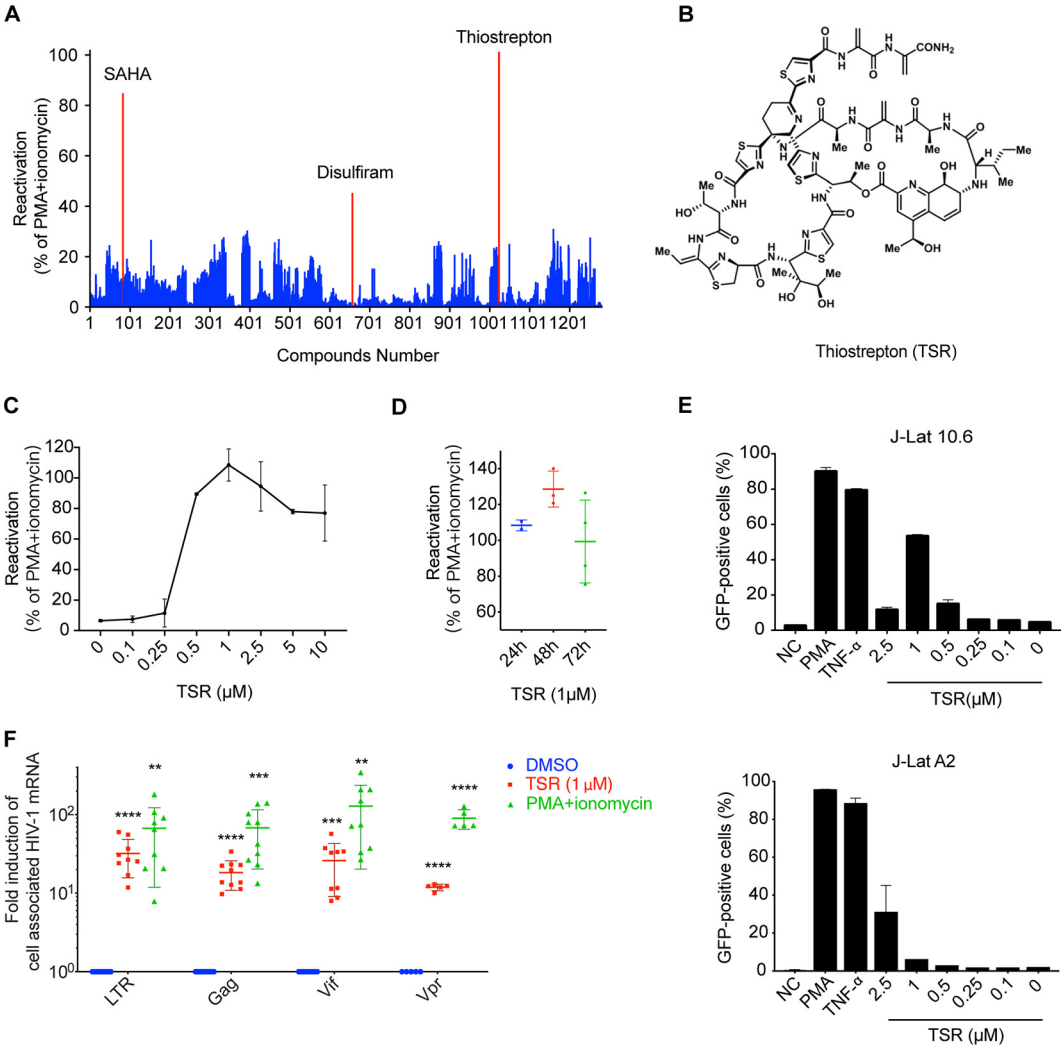

FIG 1 TSR induces latent-HIV-1 reactivation *in vitro* and *ex vivo*. (A) Summary of results of screening compounds from the U.S. Drug Collection library in a primary CD4$^+$ T cell model of HIV-1 latency. The working concentration of all compounds was 2 μM. After 72 h of treatment, reactivation efficiency was measured by flow cytometry as the percentage of GFP$^+$ cells and was normalized to the reactivation level of 50 ng/ml PMA and 1 μM ionomycin. Each bar represents the average value of triplicates. (B) Chemical structure of thiostrepton. (C) Effects of TSR on latently infected Bcl-2-transduced CD4$^+$ T cells at the indicated concentrations. (D) Effects of TSR on latently infected Bcl-2-transduced CD4$^+$ T cells at the indicated time points. (E) Effects of TSR on J-Lat 10.6 cells and J-Lat A2 cells at the indicated concentrations. (F) TSR induced latent HIV-1 expression in CD4$^+$ T cells from individuals with suppressive ART *ex vivo*. HIV-1 transcription was measured by RT-qPCR using primers specific for the LTR ($n = 9$), Gag ($n = 10$), Vif ($n = 9$) or Vpr ($n = 5$). Fold inductions are shown relative to values for the DMSO control. All data are means ± SD. Significance relative to the DMSO control value is indicated as follows: **, $P < 0.01$; ***, $P < 0.001$; ****, $P < 0.0001$.

working concentration of 1 μM (Fig. 2A). A Cell Counting Kit-8 (CCK-8) assay reflected a similar level of cytotoxicity at 1 μM, and the 50% lethal dose (LD_{50}) was around 5 μM (Fig. 2B and C). Since 1 μM TSR balanced reactivation efficiency and cytotoxicity, we used 1 μM as the working concentration for further studies. Some LRAs cause global T cell activation and induce a "cytokine storm," which limits their clinical application. We found that TSR did not significantly upregulate the expression of the T cell activation markers CD25, CD69, and HLA-DR, which is comparable to disulfiram and SAHA (Fig. 2D). The susceptibility of CD4$^+$ T cells to HIV-1 is closely related to the expression of the surface HIV-1 coreceptor CCR5 or CXCR4. Similar to disulfiram and SAHA, TSR did not change the expression of CCR5 or CXCR4 (Fig. 2E), suggesting that TSR would not increase the susceptibility of target cells to HIV-1.

CTLs play an important role in eliminating reactivated reservoir cells (28). We tested whether TSR impaired the function of CD8$^+$ T cells. TSR did not exert significant

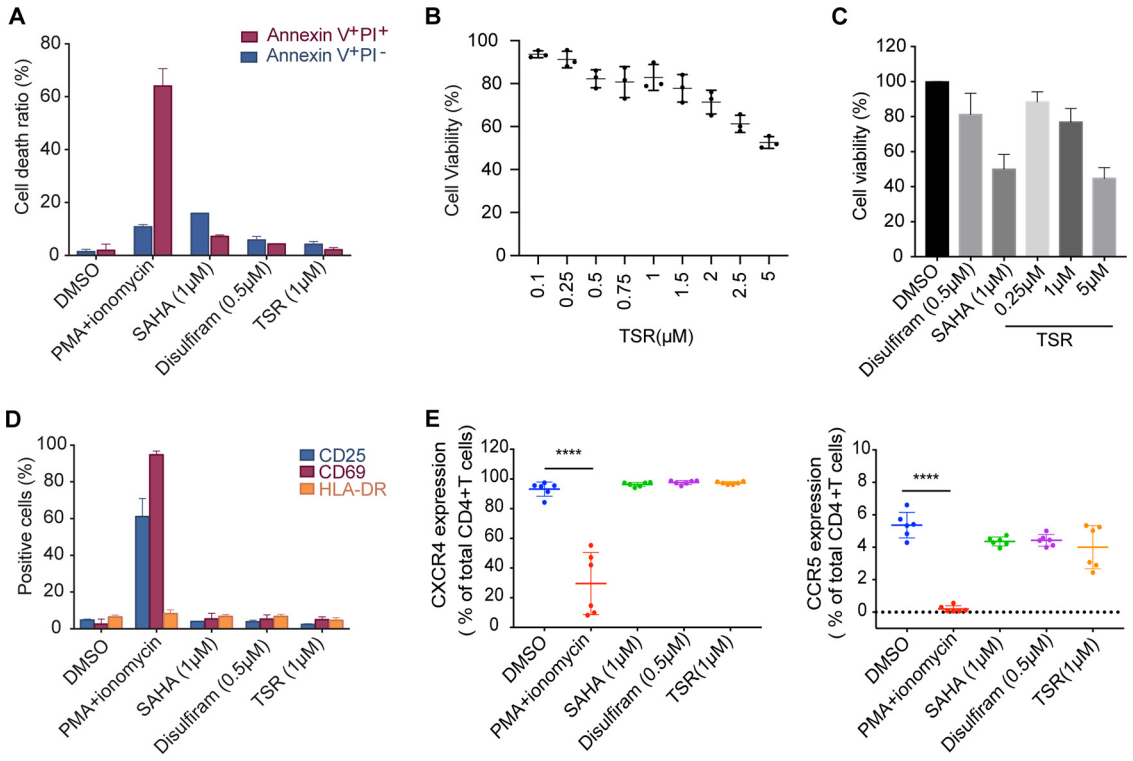

FIG 2 TSR treatment does not lead to severe cytotoxicity, global T cell activation, or coreceptor upregulation. PBMCs were isolated from healthy donors ($n = 3$ [A, B, C, and D]; $n = 6$ [E]) and treated with different groups of compounds for 48 h. (A) TSR has minimal cytotoxicity in $CD4^+$ T cells. Apoptotic cells were labeled by annexin V-PI double staining, and the percentage of positive cells in each population is shown for each concentration. (B and C) Cell viability is maintained after the indicated treatment. Cell viability was measured with a CCK-8 assay. (D) TSR does not cause T cell activation. Surface expression of CD25, CD69, and HLA-DR was detected by flow cytometry, and the percentages of positive cells are shown. (E) TSR does not upregulate HIV-1 coreceptor expression. CXCR4 (left) and CCR5 (right) expression on total $CD4^+$ T cells was analyzed by flow cytometry. ****, $P < 0.0001$ versus the DMSO control. All data are means ± SD.

cytotoxicity for $CD8^+$ T cells (see Fig. S1A in the supplemental material). PD-1 expression was slightly elevated 24 h after TSR treatment and then was quickly decreased after 48 h and 72 h. TSR treatment showed the lowest PD-1 expression compared with other groups at 72 h (see Fig. S1B). We also measured the effects on short-term $CD8^+$ T cell cytokine and lytic molecule production. TSR did not have a significant effect on CD107a, granzyme B, interferon gamma (IFN-γ), or tumor necrosis factor alpha (TNF-α) production compared to other LRAs (see Fig. S1C). Together, these results demonstrated that TSR was highly effective at reactivating latent-HIV-1 expression in both cellular models and patient-derived primary $CD4^+$ T cells *ex vivo*, without causing global T cell activation, severe cytotoxicity, or $CD8^+$ T cell dysfunction, making it a viable candidate for HIV-1 latency reversal.

TSR analogues also exhibit latency reversal activities, and TSR shows a good synergistic effect when combined with other LRAs. Nine TSR analogues with good antibacterial activity and good water solubility (29–31) were tested for their latency reversal activities. Of these, THIO-01, THIO-02, THIO-03, THIO-05, THIO-08, and THIO-09 showed more effective reactivation than 1 μM TSR following 48 h of treatment in latently infected primary $CD4^+$ T cells (Fig. 3A) or J-Lat 10.6 cells (Fig. 3B). The ability of TSR and its analogues to reactivate latent HIV-1 was further assessed by using $CD4^+$ T cells from 5 infected individuals with ART-induced suppression. One micromolar TSR, 0.5 μM THIO-01, and 1 μM THIO-08 all induced cell-associated HIV-1 RNA transcription efficiently *ex vivo* (54.68-, 96.21-, and 33.84-fold induction, respectively, compared to the DMSO control) (Fig. 3C). Interestingly, THIO-01 worked even better than the positive control (PMA-ionomycin). These results suggest that TSR and its compound family may have a similar intrinsic mechanism for reactivating latent HIV-1.

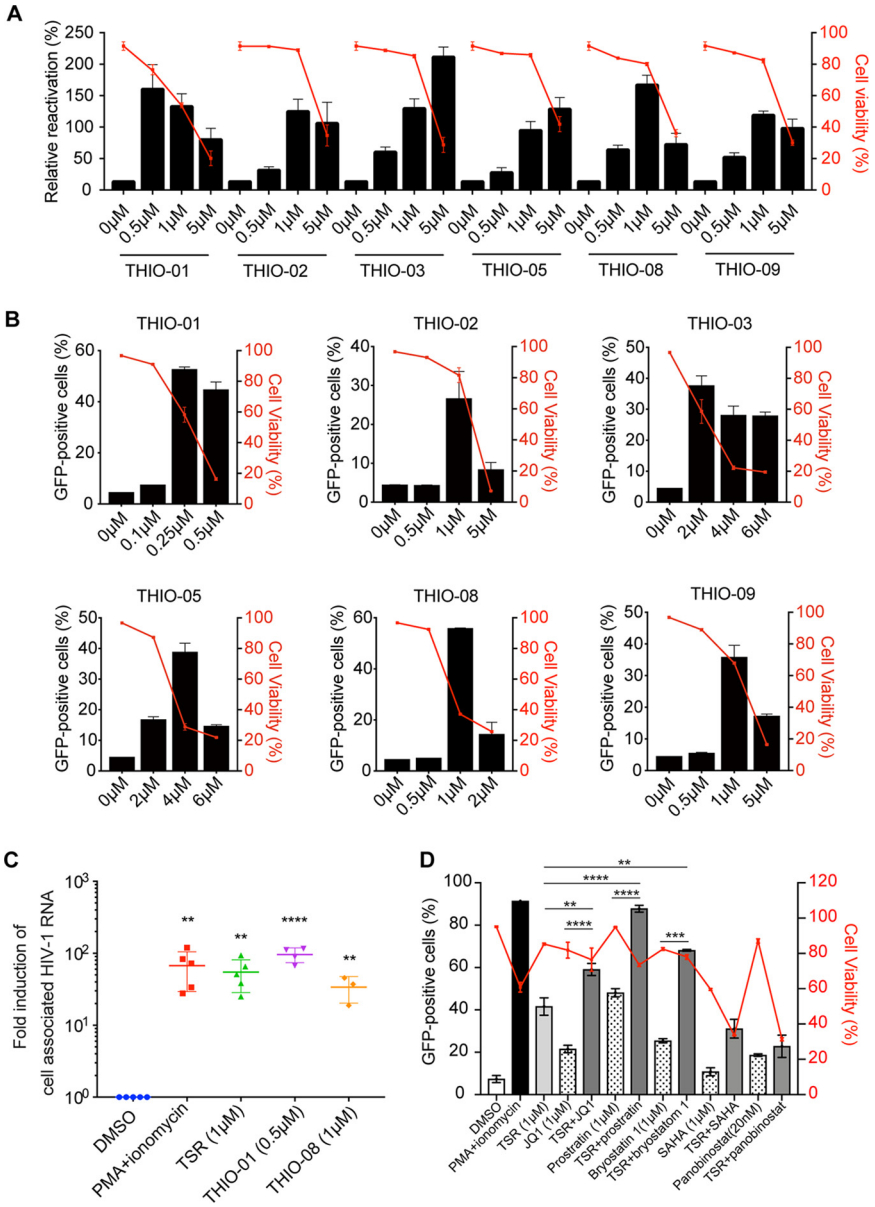

FIG 3 TSR analogues exhibit latency reversal activities, and TSR shows a good synergistic effect in combination with other LRAs. (A) Effects of TSR analogues on latently infected Bcl-2-transduced CD4$^+$ T cells. Reactivation efficiency by TSR analogues for 48 h was measured by flow cytometry as the percentage of GFP$^+$ cells and was normalized to the response to 1 μM TSR. Cell viability was measured by forward-scatter versus side-scatter gating. (B) Effects of TSR analogues on J-Lat 10.6 cells after 48 h. Reactivation was measured by flow cytometry as the percentage of GFP$^+$ cells. (C) TSR induced latent HIV-1 transcription in CD4$^+$ T cells from infected individuals with suppressive ART *ex vivo*. HIV-1 transcription was measured by HIV-1 viral quality assurance assay. Fold inductions are shown relative to DMSO. Significance relative to DMSO control values is indicated as follows: **, $P < 0.01$; ****, $P < 0.0001$. (D) Combinatory effects of TSR and other LARs on J-Lat 10.6 cells. Reactivation and cell viability were measured by flow cytometry using the indicated compounds or combinations for 48 h. Significance relative to values for TSR or other LRA treatment alone is indicated as follows: **, $P < 0.01$; ***, $P < 0.001$; ****, $P < 0.0001$. All data are means ± SD.

It has been suggested that latency reversal with a single LRA may not be enough and that a combination of LRAs may be needed to fully activate latent HIV-1 (32). In addition, single LRAs have not shown complete effectiveness in clinical trials so far (26, 33). To further verify the latency-reversing activity of TSR and to evaluate its potential to act in combination with other LRAs, we performed an LRA combination experiment in J-Lat 10.6 cells. Apparent synergistic effects were observed when TSR was combined

with JQ1, prostratin, or bryostatin-1 (Fig. 3D). However, there was no advantage when TSR was combined with the HDAC inhibitor SAHA or panobinostat (Fig. 3D).

TSR upregulates heat shock proteins in CD4$^+$ T cells. In order to decipher the mechanisms underlying latent HIV-1 reactivation by TSR, we performed transcriptome sequencing (RNA-Seq) to identify genes that were modulated by TSR versus DMSO treatment in CD4$^+$ T cells. Genome-wide transcriptional profiling revealed that a series of HSP mRNAs were significantly upregulated in latently infected Bcl-2-transduced CD4$^+$ T cells or primary CD4$^+$ T cells, especially HSP90 and HSP70 (HSPA1A and HSPA1B) (Fig. 4A). KEGG pathway analysis showed totally different expression patterns for genes regulated by TSR and PMA (Fig. 4B). Our data support the previous report that TSR binds ribosomal protein (34), induces ER stress, and upregulates HSPs by inhibiting proteasome (16, 19). RNA-Seq data were further confirmed in latently infected, Bcl-2-transduced CD4$^+$ T cells. HSP RNA transcription was significantly upregulated by TSR (Fig. 4C, left), and HSP70 and HSP90 protein expression was also elevated upon TSR or MG132 treatment (Fig. 4C, right). In J-Lat 10.6 cells, similar results were observed at both the RNA level and the protein level (Fig. 4D). HSF1 is the primary transcription factor responsible for the activation of heat shock response (HSR) to different forms of cellular stresses (35). We observe that RNA expression of HSPs decreased when cells were cotreated with the HSF1 inhibitor KRIBB11 (Fig. 4D). We confirmed that HSF1 knockdown downregulated RNA transcription of both HSP70 and HSP90 (see Fig. S2A in the supplemental material). Together, these results revealed that TSR triggered the heat shock response in CD4$^+$ T cells, which was dependent on HSF1, suggesting that HSPs may have a role in latent HIV-1 reactivation by TSR.

TSR-mediated latent HIV-1 reactivation depends on HSF1, HSP70, and HSP90. Recent evidence has suggested that HSP70 and HSP90 regulate HIV-1 transcription (21–23). Proteasome inhibitors such as MG132, CFZ, and BTZ were shown to induce latent HIV-1 reactivation dependent on HSF1 activation (20). To verify that HSF1, HSP70, and HSP90 participate in TSR-mediated latent HIV-1 reactivation, we carried out inhibition assays with TSR and various HSR inhibitors (HSF1 inhibitor KRIBB11, HSP90 inhibitors 17AAG and AUY922, and HSP70 inhibitor VER155008). We found that the latency reversal activity of TSR was inhibited by KRIBB11, 17AAG, AUY922, and VER155008 (Fig. 5A; also, see Fig. S3). The protein levels of HSF1 and p-HSF1(Ser-326) were upregulated by TSR and abolished by KRIBB11 cotreatment in a dose-dependent manner (Fig. 5B). Nuclear translocation of HSF1 is an important regulatory step for its activation (36). We observed that TSR induced a significant increase of HSF1 nuclear translocation in J-Lat 10.6 cells (Fig. 5C). Using short hairpin RNA (shRNA) (knockdown of HSF1, HSP70, or HSP90) in J-Lat 10.6 cells further confirmed their functions in TSR-mediated HIV-1 latency reversal. Knockdown efficiency was confirmed by qPCR and Western blotting (see Fig. S2). In comparison to wild-type J-Lat 10.6 cells, HSF1, HSP70, or HSP90 knockdown significantly impaired latent HIV-1 reactivation induced by TSR (Fig. 5D). Therefore, our results demonstrated that the heat shock response is critical in TSR-mediated HIV-1 latency reversal.

TSR reactivates HIV-1 through the NF-κB and p-TEFb pathways. To further verify which downstream signaling pathway of heat shock response directly drives latent HIV-1 transcription, we utilized specific inhibitors to block pathways known for their transcriptional activities on HIV-1. Our data revealed that NF-κB inhibitor (Bay11-7082) and p-TEFb inhibitor (DRB) had a significant inhibitory effect on TSR-mediated latent HIV-1 reactivation in a dose-dependent manner (Fig. 6A; also, see Fig. S3), while a PKC inhibitor (Go6983) and an NFAT (nuclear factor of activated T cells) inhibitor (cyclosporine) did not have any effect. In agreement with viral protein expression, TSR upregulated the expression of corresponding proteins (p65 and CDK9) and Bay11-7082 or DRB abolished TSR's effect in J-Lat 10.6 cells (Fig. 6B and C). It is well known that migration of the p65/p50 complex into the nucleus is a key step of NF-κB activation (37). We found that the nuclear localization signal of p65 was significantly elevated following TSR treatment (Fig. 6D), confirming that the NF-κB pathway was activated by TSR. In

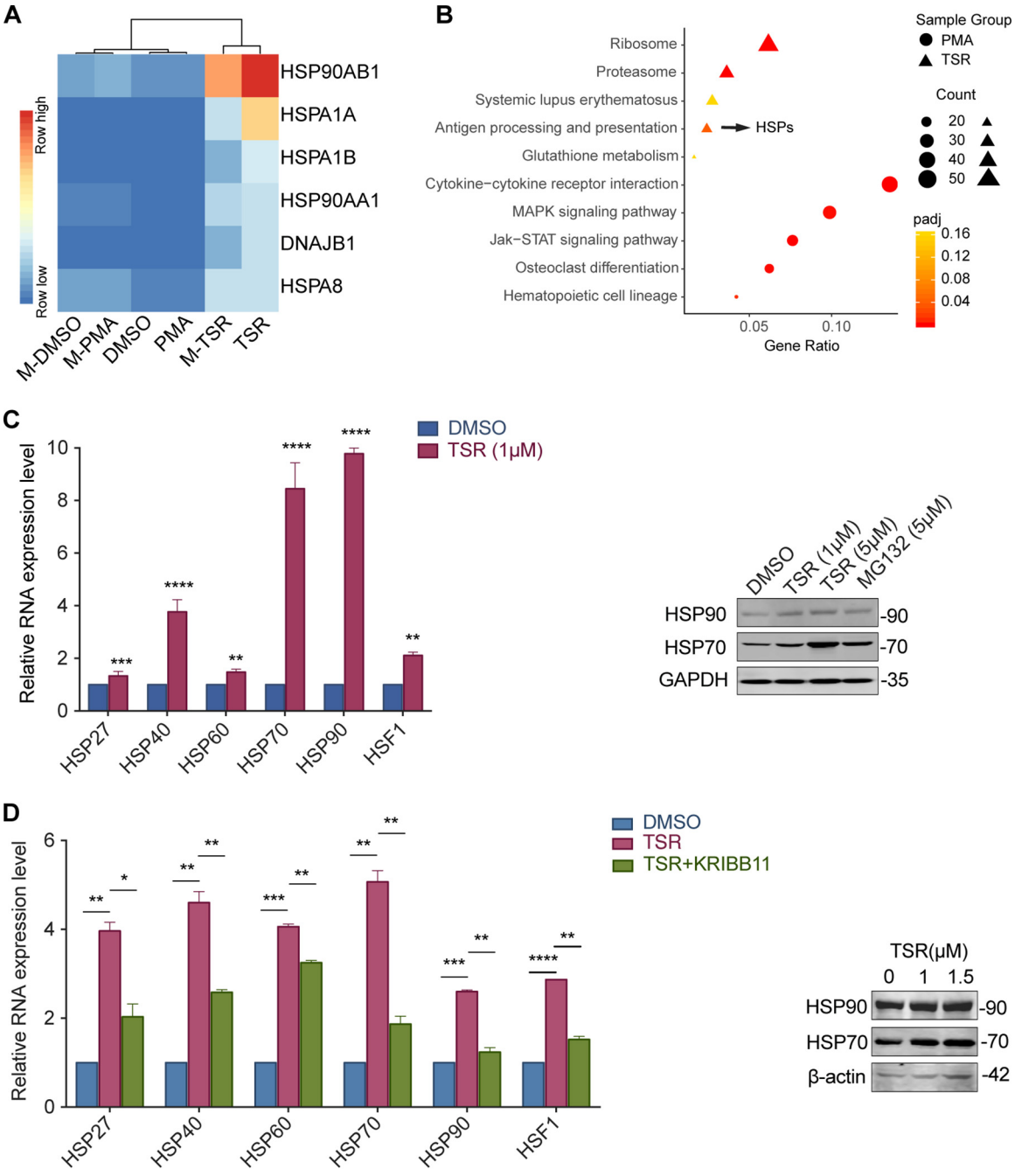

FIG 4 TSR upregulates heat shock proteins in CD4$^+$ T cells. (A) HSP gene transcription was upregulated after TSR treatment. CD4$^+$ T cells from healthy donors and latently infected Bcl-2-transduced CD4$^+$ T cells (M, Bcl-2 model) were treated with DMSO, TSR, or PMA for 72 h; total RNA was then subjected to RNA-Seq. A heat map of HSP gene transcription is shown. (B) Enrichment plots depict KEGG pathways upmodulated by TSR or PMA versus the DMSO control. (C and D) TSR upregulated HSP expression. Latently infected Bcl-2-transduced CD4$^+$ T cells (C) or J-Lat 10.6 cells (D) were treated with DMSO, TSR, or TSR-KRIBB11 for 24 h. RNA transcription was detected by qPCR (C and D, left). Graphs show relative expression of the indicated genes compared to the DMSO control, which was set at 1. HSP70 and HSP90 were measured by Western blotting (C and D, right). For panels A and B, the R package DEGseq was used, and the differentially expressed genes (DEGs) were identified based on a $\log_2$ fold change value of ≥1 and a P value of ≤0.05. (C and D) Significance relative to the DMSO control is indicated as follows: *, $P < 0.05$; **, $P < 0.01$; ***, $P < 0.001$; ****, $P < 0.0001$. All data are means ± SD.

comparison to wild-type J-Lat 10.6 cells after TSR treatment, HSF1, HSP70, or HSP90 knockdown significantly reduced the p65 (Fig. 6D) and CDK9 (Fig. 6E) nuclear localization signals. Together, our data clearly indicated that NF-κB and p-TEFb are downstream of the heat shock response in the signaling pathway underlying TSR-mediated latency reversal.

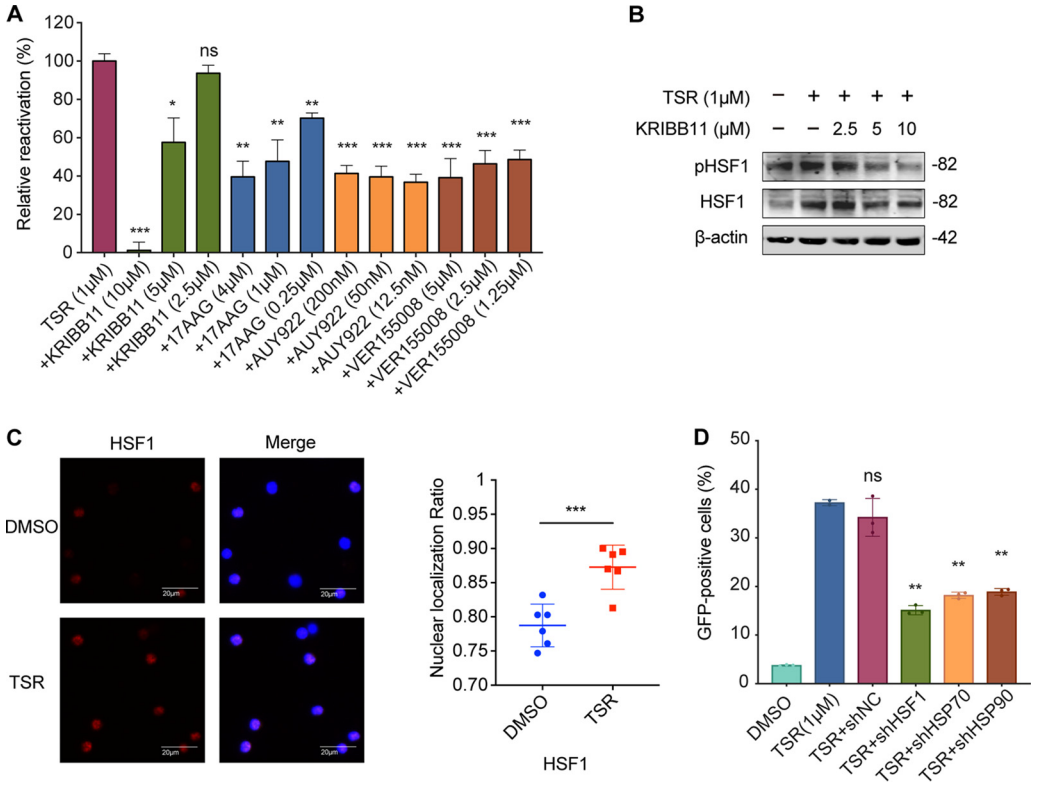

FIG 5 TSR-mediated latent HIV-1 reactivation depends on HSF1, HSP70, and HSP90. (A) HSP-specific inhibitors counteract latency reversal by TSR. TSR was used alone or was combined with inhibitors on latently infected Bcl-2-transduced CD4$^+$ T cells for 48 h at the indicated concentrations. The percentage of GFP$^+$ cells was measured by flow cytometry and was normalized to the response to 1 μM TSR treatment. Significance relative to TSR alone is indicated as follows: *, $P < 0.05$; **, $P < 0.01$; ***, $P < 0.001$; ****, $P < 0.0001$. (B) KRIBB11 counteracts TSR-mediated upregulation of HSF and pHSF1. J-Lat 10.6 cells were treated with TSR alone or together with KRIBB11 at the indicated concentrations for 2 h. Levels of the corresponding proteins were measured by Western blotting. (C) HSF-1 nuclear localization increases after TSR treatment. J-Lat 10.6 cells were treated with 1 μM TSR for 2 h. HSF1 immunofluorescence staining was performed (C, left). Pearson's correlation coefficient reflects nuclear localization of HSF1 (C, right). ***, $P < 0.001$ versus DMSO control. (D) Knockdown of HSF1, HSP70, or HSP90 reduces TSR-mediated latent HIV-1 reactivation. shRNAs of HSF1, HSP70, and HSP90 were transduced into J-Lat 10.6 cells. The percentage of GFP$^+$ cells after knockdown was measured by flow cytometry after 1 μM TSR treatment for 36 h. **, $P < 0.01$ versus the TSR (1 μM) group. All data are means ± SD.

DISCUSSION

The presence of an extremely stable viral latent reservoir in infected individuals is considered the main obstacle to curing HIV-1 infection. Finding efficient, safe, and highly viable LRAs or suitable combinations is critical to viral eradication. Previously reported LRAs, such as histone deacetylase inhibitors, p-TEFb activators, and PKC activators, have achieved good reactivation *in vitro* and *ex vivo*, but little reduction of the latent reservoir was observed in clinical trials (26, 38). It is still urgent to discover novel, effective, and safe LRAs or to optimize the potential ability of the existing LRAs. Here, by taking advantage of a previously described primary cell model (24), we screened more than 1,280 FDA-approved compounds and successfully identified TSR as a highly efficient LRA.

Besides its antibiotic effects, TSR is also known for its potential to inhibit cancer cells (15, 17). Currently, there are three proteasome inhibitors approved by the FDA to treat multiple myeloma or mantle-cell lymphoma in clinical trials: BTZ, CFZ, and ixazomib (39). Some proteasome inhibitors have been reported for their ability to induce latent HIV-1 reactivation (20), and the effect of ixazomib on the latent HIV-1 reservoir is being evaluated in a clinical trial (NCT02946047). Therefore, proteasome inhibitors, including TSR, will be a promising drug class of great clinical significance in future applications. TSR analogues and a large synergistic effect with other LRAs also improve TSR's value

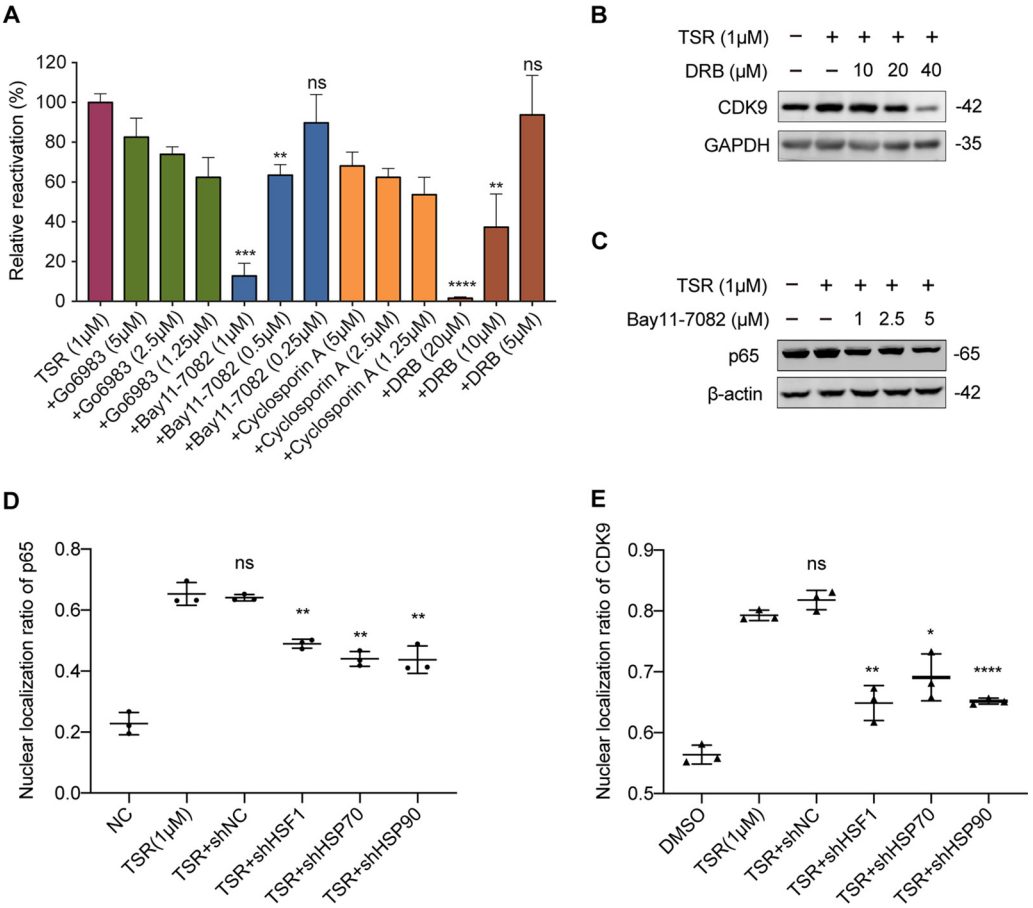

FIG 6 TSR reactivates HIV-1 through the NF-κB and p-TEFb pathway. (A) Inhibitors of the NF-κB and p-TEFb pathway affect TSR-mediated latency reversal. Latently infected Bcl-2-transduced CD4$^+$ T cells were treated with TSR alone or with specific inhibitors for 48 h at the indicated concentrations. The percentage of GFP$^+$ cells was measured by flow cytometry and was normalized to the response to 1 μM TSR treatment. Significance relative to TSR alone is indicated as follows: *, $P < 0.05$; **, $P < 0.01$; ***, $P < 0.001$; ****, $P < 0.0001$. (B and C) p-TEFb and NF-κB inhibitors reduce the corresponding signaling pathway. J-Lat 10.6 cells were treated with TSR alone or with DRB (B) or Bay11-7082 (C) at the indicated concentrations for 24 h. The expression of the corresponding proteins was measured by Western blotting. (D and E) Knockdown of HSF1, HSP70, or HSP90 decreases nuclear signal after TSR treatment. J-Lat 10.6 cells were treated with 1 μM TSR for 5 h. Pearson's correlation coefficient reflects the p65 (D) or CDK9 (E) nuclear localization ratio. Significance relative to the TSR (1 μM) group is indicated as follows: *, $P < 0.05$; **, $P < 0.01$; ****, $P < 0.0001$. All data are means ± SD.

for clinical application. However, which functional group(s) in these TSR analogues is crucial to the mechanism of latent HIV-1 reactivation needs to be further explored.

It has been reported that TSR induces ER stress in promoting tumor cell apoptosis and then initiates the heat shock response to maintain intracellular homeostasis (19, 40). Our studies showed that TSR triggered significant upregulation of HSPs in CD4$^+$ T cells and induced HIV-1 transcription subsequently through the NF-κB and p-TEFb pathway, combining mechanisms of transcriptional initiation and elongation, which may lead to an optimal reactivation. HSF1 is a master regulator of HSPs by binding heat shock elements (HSEs) upstream of heat shock genes (41). Previous reports have suggested that phosphorylated HSF1 interacts with the HSE domain in the HIV-1 5′ LTR and positively regulates HIV-1 expression (42). Our data further solidify the important role of HSF1 in reactivating latent HIV-1 transcription.

The molecular chaperone HSP70 and the kinase-specific chaperone HSP90/Cdc37 were implied to act on the stabilization and folding of Cdk9 and the assembly of the Cdk9-cyclin T1 complex responsible for the p-TEFb-mediated Tat activation of HIV-1 transcription (23). HSP70 binding protein 1 (HspBP1), an HSP70 cochaperone, was identified as a host-intrinsic inhibitor of HIV-1. HspBP1 was recruited to the NF-κB

enhancer domain on the HIV-1 LTR, which impeded the binding of p50/p65 (36). We hypothesize that the increased expression of HSP70 triggered by TSR may rescue the inhibition of HIV-1 transcription by HspBP1 through competitive binding.

HSP90 expression was also regulated by NF-κB. Evidence indicated that NF-κB binding to the 5′-flanking region of the HSP90 promoter would upregulate HSP90 (43). The HSP90 inhibitor 17AAG reduced the degradation of IκBα and blocked nuclear translocation of p65/p50, which eventually suppressed the NF-κB pathway. However, the role of active NF-κB signaling in regulating HSP90 or other HSPs in HIV-1-infected cells is still unclear and warrants further investigation.

In summary, our study has reported a novel LRA, TSR, which is effective in activating latent HIV-1 transcription without causing global T cell activation. TSR has minimal toxicity, does not increase the susceptibility of target cells to HIV-1, and does not induce $CD8^+$ T cell dysfunction, making it a promising new compound for future applications aiming to reduce the reservoir of latent HIV-1.

MATERIALS AND METHODS

Study approval. The use of peripheral blood mononuclear cells (PBMCs) from healthy adult donors was approved by the Institutional Review Board of Guangzhou Blood Center (Guangzhou, Guangdong, China). PBMCs from HIV-1-infected patients were collected at The Fifth Affiliated Hospital of Sun Yat-sen University (Zhuhai, Guangdong, China). This study was approved by the Ethics Review Boards of The Fifth Affiliated Hospital of Sun Yat-sen University (2018K41-1). All human participants provided written informed consent for their participation in the study and agreed with the publication of the scientific results.

Cell culture. J-Lat 10.6 cells and J-Lat A2 cells were originally generated in Eric Verdin's laboratory (The Buck Institute for Research on Aging, Novato, CA) and were obtained from Robert F. Siliciano's laboratory (Department of Medicine, Johns Hopkins University School of Medicine, Baltimore, MD). PBMCs from healthy adult donors were provided by the Guangzhou Blood Center (Guangzhou, Guangdong, China), The ages of the HIV-negative donors included in our study ranged from 18 to 65 years. CD4 and CD8 counts were in the normal range of clinical test values, and none of the donors was infected with HIV-1. PBMCs from HIV-1-infected individuals were collected in The Fifth Affiliated Hospital of Sun Yat-sen University (Zhuhai, Guangdong, China). HIV-1-infected individuals were selected based on sustained suppression of plasma viral load (plasma viral loads of $<$50 copies/ml) for at least 12 months and a CD4 count of $>$400 cells/μl. Their essential information is provided in Table S1 in the supplemental material. PBMCs were isolated by density gradient centrifugation using Ficoll (TBDscience). All the J-Lat cell lines and PBMCs were cultured in RPMI 1640 (Gibco) supplemented with 1% penicillin-streptomycin and 10% fetal bovine serum (FBS) (Gibco).

Generation of a Bcl-2-transduced primary $CD4^+$ T cell model. The protocol used is from Robert F. Siliciano's lab (Department of Medicine, Johns Hopkins University School of Medicine, Baltimore, MD) (24). Briefly, primary $CD4^+$ T cells were isolated from PBMCs with a human $CD4^+$ T lymphocyte enrichment set (Becton Dickinson, USA) according to the manufacturer's instructions, and purity was $>$95%. $CD4^+$ T cells were costimulated with anti-CD3 and anti-CD28 antibodies (BioLegend) and were transduced with the Bcl-2 expression vector EB-FLV at a multiplicity of infection (MOI) of 5 to 10 by spinoculation at 1,200 $\times$ *g* at room temperature for 2 h. Following 3 to 4 weeks of culture, viable cells were isolated using Ficoll density gradient centrifugation. We then infected activated Bcl-2-transduced cells with reporter virus NL4-3-Δ6-drEGFP at an MOI of less than 0.1. We maintained the infected cells in interleukin 2 (IL-2)- and T cell growth factor-enriched medium for 3 days after infection. We then incubated the infected cells in RPMI 1640 with 10% fetal bovine serum (FBS) and 1% penicillin-streptomycin without exogenous cytokines for more than 1 month. Finally, we isolated the GFP^- cells to more than 99.9% purity using fluorescence-activated cell sorting (FACSAria II; Becton Dickinson). NL4-3-Δ6-drEGFP and EB-FLV were gifts from Robert F. Siliciano's laboratory.

High-throughput drug screening. Latently infected cells (1×10^5) were resuspended in 200 μl of medium (RPMI 1640 with 10% FBS and 1% penicillin-streptomycin) and were cultured in round-bottom 96-well plates. The cells were then treated with different compounds at 2 μM. As a positive control, cells were treated with 50 ng/ml PMA and 1 μM ionomycin. After 72 h of cell culture at 37°C, reactivation of latent HIV-1 was determined by quantifying the percentage of GFP^+ cells using the standard mode of the high-throughput sampler in LSRFortessa and analyzed using Plate Manager (BD Biosciences). The percentage of GFP^+ cells was normalized based on the response to 50 ng/ml PMA and 1 μM ionomycin.

Flow cytometry analysis. After treatment, cells were collected to calculate the percentage of GFP^+ cells and determine the level of HIV gene expression by flow cytometry through the fluorescein isothiocyanate (FITC) channel (LSRFortessa; Becton Dickinson). Surface staining was performed with fluorochrome-conjugated antibodies, including CD3-BV421 (OKT3), CD4-APC-Cy7 (OKT4), CD8-peridinin chlorophyll protein (PerCP) (RPA-T8), CD25-phycoerythrin (PE) (BC69), CD69-FITC (FN50), HLA-DR-PE dazzle 594 (L243), PD-1–PE (EH12.2H7), CD107a-allophycocyanin (APC) (H4A4), CXCR4-PE-Cy7 (12G5), and CCR5-APC (J418F1). Intracellular staining was subsequently performed with granzyme B-AF647 (GB11), IFN-γ–BV605 (4S.B3), and TNF-α–APC (MAb 11) antibodies (BioLegend). The fluorescence value was analyzed by FlowJo (version 10.4.0).

qPCR. Cells were incubated with different drugs for different time intervals. Total RNA was extracted using TRIzol (Invitrogen) and chloroform and then precipitated with isopropyl alcohol. RNA reverse transcription to cDNA was done according to the procedure for the SuperScript IV system control reactions (Thermo Fisher). Quantitative PCR was performed using SYBR qPCR master mix (Vazyme) on a QuantStudio 3 PCR system (Thermo Fisher) using a standard two-step procedure (denatured at 95°C for 10 s and annealed-extended at 60°C for 30 s; 40 cycles). RT-PCR primer sequences are shown in Table S2 and are consistent with a previous report (44). The $2^{-\Delta\Delta CT}$ method was adopted to analyze the relative expression of mRNAs, using the GAPDH (glyceraldehyde-3-phosphate dehydrogenase) gene as the reference gene.

Viral quality assurance. Total cellular RNA was extracted from 1 million CD4$^+$ T cells after 24 h of stimulation followed by reverse transcription. Real-time PCR was performed using the TaqMan (Life Technologies) gene expression assay. HIV-1 mRNAs were detected using the following primers and probe (modified from the work of Shan et al. [44]): forward (5′→3′), CAGATGCTGCATATAAGCAGCTG (9501 to 9523); reverse (5′→3′), TTTTTTTTTTTTTTTTTTTTTTTTGAAGCAC [9629 to the poly(A) tail]; probe (5′→3′), 6-carboxyfluorescein (FAM)-CCTGTACTGGGTCTCTCTGG-MGB (9531 to 9550), The cycling parameters were as follows: 2 min at 50°C, 10 min at 95°C, and 45 to 50 cycles at 95°C for 15 s and then 60°C for 60 s. Molecular standard curves were generated using serial dilutions of a TOPO plasmid containing the last 352 nucleotides of viral genomic RNA plus 30 deoxyadenosines (pVQA). Results for each drug treatment are presented as fold change relative to the DMSO control (means ± standard deviations [SD]).

Cytotoxicity assays. The cell death ratio was evaluated by an annexin V-PI double staining assay. The cells were incubated with annexin V-FITC at room temperature for 15 min, PI was added, and the stained cells were analyzed by flow cytometry. Cell viability was measured with CCK-8 (MedChemExpress). PBMCs were plated at 1×10^6 cells per well in a 96-well plate and incubated with drugs for 48 h. Then, 10 μl of CCK-8 reagent was added to 100 μl of cell culture mixture and incubated for an additional 4 h. Optical density (OD) was recorded at a wavelength of 450 nm on a microplate reader (Molecular Devices). The cell viability was calculated as follows: $[(OD_{treated} - OD_{blank\ control})/(OD_{untreated} - OD_{blank\ control})] \times 100$.

RNA-Seq. Freshly isolated CD4$^+$ T cells and latently infected, Bcl-2-transduced CD4$^+$ T cells were stimulated with DMSO, PMA, or TSR for 2 days. Total RNA from each group was extracted with TRIzol reagent and quantified using a Nanodrop 2000 spectrophotometer (Thermo Fisher). The RNA quality was determined using the Agilent 2100 bioanalyzer. The RNA-Seq library was built with a TruSeq stranded mRNA library prep kit (Illumina) and sequenced with HiSeq X Ten (Illumina) at Novogene (Beijing, China). Raw reads from the RNA-Seq data were quality-controlled by the FastQC tool and trimmed using Trimmomatic (48) for the removal of adapter and low-quality sequences. The resulting clean reads were mapped to human reference genome NCBI build 38 (GRCh38) by Hisat2 (45) with default parameters. Gene expression levels were calculated using the Stringtie software based on the number of reads per kilobase per million mapped reads (RPKM). Differentially expression analysis was performed using the R package DEGseq, and the differentially expressed genes (DEGs) were identified based on a $\log_2$ fold change value of ≥1 and a P value of ≤0.05. The DEG expression levels were visualized with a heat map or scatter plot by using the R package gplots.

Western blotting. After treatment, cells were lysed in radioimmunoprecipitation (RIPA) lysis buffer (10 mM Tris-HCl buffered at pH 7.5, 150 mM NaCl, 0.5% NP-40, 1% Triton X-100, 10% glycerol, 2 mM EDTA, 1 mM NaF, 1 mM Na_3VO_4, 1× protease and phosphatase inhibitor cocktail) and incubated on ice for 30 min, followed by centrifugation at 12,000 × g for 10 min at 4°C. The supernatants were collected as a whole protein extract. Protein samples were stored at −80°C or directly used for Western blotting. The protein extract was denatured by addition of NuPAGE running buffer (Thermo Fisher), followed by denaturation at 100°C for 10 min, and 50 μg of total protein was subjected to electrophoresis for 1.5 h on a 10% polyacrylamide gel to separate the proteins, transferred onto polyvinylidene difluoride (PVDF) membranes (Bio-Rad), and coincubated with primary and secondary antibodies. The antibodies were diluted with 5% bovine serum albumin (BSA). Subsequently, blots were imaged on an infrared (IR) laser-based fluorescence imaging system (LI-COR Odyssey).

Immunofluorescence. CD4$^+$ T cells (1×10^6/ml) were isolated by magnetic activated cell sorting and then plated on a Lab-Tek II chambered cover glass (Thermo Fisher) which had been pretreated with poly-lysine (Sigma-Aldrich). Twelve hours later, cells were treated with DMSO or TSR for another 2 h. The coverslips were washed once with 1× phosphate-buffered saline, and bound cells were fixed in 4% formaldehyde for 15 min at room temperature. Fixed cells were permeabilized by sequential treatments with 0.2% Triton X-100 (Sigma-Aldrich) for 10 min followed by 1× Perm/Wash buffer (Becton Dickinson) for 30 min. After blocking with 10% normal goat serum (Boster) for 15 min, cells were immunostained for 2 h at room temperature with primary antibodies against HSF1 and p65. Then, the cells were washed three times with 1× Perm/Wash buffer and incubated with a 1:100 dilution of Cy3-conjugated anti-rabbit IgG secondary antibody (Sigma-Aldrich) for 1 h. After the coverslips had been washed with 1× Perm/Wash buffer, they were counterstained with 1 μg/ml DAPI (Sigma-Aldrich) and mounted onto glass slides with ProLong antifade (Thermo Fisher). Fluorescent images were captured with a Leica DM6B microscope. Nuclear and cytoplasmic localization were analyzed with ImageJ.

shRNA-mediated knockdown. shRNA targeting luciferase (shluc; 5′-ACCGCCTGAAGTCTCTGATTAA-3′) was set as the negative control (46). The shRNA target sequence specific for the coding sequence is shown in Table S3. Target sequences were cloned into pLKO.3G-RFP, which was derived from pLKO.3G (Addgene plasmid number 14748). The GFP tag was replaced with a red fluorescent protein (RFP) tag in pLKO.3G-RFP. Pseudotyped viral stocks were produced in HEK293T cells by cotransfecting 2.2 μg of vesicular stomatitis virus glycoprotein (VSV-G) expression vector, 4.4 μg of lentiviral packaging construct

pCMVDR8.2, and 4.4 μg of an shRNA expression lentiviral construct using Lipofectamine 2000 (Thermo Fisher) according to the manufacturer's instruction. The VSV-G expression vector was obtained from Addgene (Addgene plasmid number 12259). pCMVDR8.2 was a kind gift from Didier Trono (School of Life Sciences, Ecole Polytechnique Fédérale de Lausanne, Lausanne, Switzerland) (47). Virus supernatants from each 10-cm dish were concentrated in 1 ml RPMI 1640 with polyethylene glycol (PEG) 6000. J-Lat 10.6 cell lines were spin-infected with the shRNA virus. The infection efficiency was measured based on the percentage of RFP-positive cells determined by flow cytometry after 48 h. The knockdown efficiency was confirmed by both qPCR and Western blotting. Infected cells were treated with TSR (Selleckchem) for another 48 h, and the percentages of GFP$^+$ cells were determined by flow cytometry and analyzed with FlowJo.

Statistics. Statistical analyses were performed with GraphPad Prism 7 (GraphPad), and a P value of <0.05 was considered significant for all comparisons. The two-tailed unpaired Student's t test was used unless otherwise specified.

Data availability. RNA-Seq data are available in the Sequence Read Archive database. The accession numbers are SRR11144590, SRR11144591, SRR11144592, SRR11144593, SRR11144594, and SRR11144595.

SUPPLEMENTAL MATERIAL

Supplemental material is available online only.

SUPPLEMENTAL FILE 1, PDF file, 0.5 MB.

ACKNOWLEDGMENTS

We appreciate all the volunteers who donated blood samples for this study. We thank Yuxia Lin and Qing Zhou for their assistance with Western blotting. We thank Xiaofan Yang, Jinfeng Cai, and Zhaoli Liu for helpful discussions.

Funding for this study was provided by the National Special Research Program of China for Important Infectious Diseases (2018ZX10302103 and 2017ZX10202102), National Natural Science Foundation of China (81672024), Natural Science Foundation of Guangdong Province of China (2017A030306005, 2016A030313325), and the Guangdong Innovative and Entrepreneurial Research Team Program (2016ZT06S638) to K.D. and by the fund from Guangzhou Institute of Pediatrics/Guangzhou Women and Children's Medical Center (1600011), the Fundamental Research Funds for the Central Universities (17ykpy03), and the Natural Science Foundation of Guangdong Province of China (2017A030310202) to D.L.

W.P., D.L., and K.D. designed experiments. W.P., D.L., X.C., H.G., and J.Z. conducted experiments. Z.H. provided clinical resources. W.L. provided TSR analogues and technical support. K.D. and D.L. financially supported the research. W.P. and K.D. wrote the manuscript, and all authors contributed to manuscript editing.

We declare that no conflict of interest exists.

REFERENCES

1. Chun TW, Finzi D, Margolick J, Chadwick K, Schwartz D, Siliciano RF. 1995. In vivo fate of HIV-1-infected T cells: quantitative analysis of the transition to stable latency. Nat Med 1:1284–1290. https://doi.org/10.1038/nm1295-1284.
2. Chun TW, Carruth L, Finzi D, Shen X, DiGiuseppe JA, Taylor H, Hermankova M, Chadwick K, Margolick J, Quinn TC, Kuo YH, Brookmeyer R, Zeiger MA, Barditch-Crovo P, Siliciano RF. 1997. Quantification of latent tissue reservoirs and total body viral load in HIV-1 infection. Nature 387:183–188. https://doi.org/10.1038/387183a0.
3. Siliciano JD, Kajdas J, Finzi D, Quinn TC, Chadwick K, Margolick JB, Kovacs C, Gange SJ, Siliciano RF. 2003. Long-term follow-up studies confirm the stability of the latent reservoir for HIV-1 in resting CD4+ T cells. Nat Med 9:727–728. https://doi.org/10.1038/nm880.
4. Strain MC, Günthard HF, Havlir DV, Ignacio CC, Smith DM, Leigh-Brown AJ, Macaranas TR, Lam RY, Daly OA, Fischer M, Opravil M, Levine H, Bacheler L, Spina CA, Richman DD, Wong JK. 2003. Heterogeneous clearance rates of long-lived lymphocytes infected with HIV: intrinsic stability predicts lifelong persistence. Proc Natl Acad Sci U S A 100:4819–4824. https://doi.org/10.1073/pnas.0736332100.
5. Crooks AM, Bateson R, Cope AB, Dahl NP, Griggs MK, Kuruc JD, Gay CL, Eron JJ, Margolis DM, Bosch RJ, Archin NM. 2015. Precise quantitation of the latent HIV-1 reservoir: implications for eradication strategies. J Infect Dis 212:1361–1365. https://doi.org/10.1093/infdis/jiv218.
6. Xing S, Siliciano RF. 2013. Targeting HIV latency: pharmacologic strategies toward eradication. Drug Discov Today 18:541–551. https://doi.org/10.1016/j.drudis.2012.12.008.
7. Richman DD, Margolis DM, Delaney M, Greene WC, Hazuda D, Pomerantz RJ. 2009. The challenge of finding a cure for HIV infection. Science 323:1304–1307. https://doi.org/10.1126/science.1165706.
8. Cary DC, Peterlin BM. 2016. Targeting the latent reservoir to achieve functional HIV cure. F1000Res 5:1009. https://doi.org/10.12688/f1000research.8109.1.
9. Deeks SG. 2012. HIV: shock and kill. Nature 487:439–440. https://doi.org/10.1038/487439a.
10. Bosque A, Planelles V. 2009. Induction of HIV-1 latency and reactivation in primary memory CD4+ T cells. Blood 113:58–65. https://doi.org/10.1182/blood-2008-07-168393.
11. Spivak AM, Planelles V. 2018. Novel latency reversal agents for HIV-1 cure. Annu Rev Med 69:421–436. https://doi.org/10.1146/annurev-med-052716-031710.
12. Jones RB, O'Connor R, Mueller S, Foley M, Szeto GL, Karel D, Lichterfeld M, Kovacs C, Ostrowski MA, Trocha A, Irvine DJ, Walker BD. 2014. Histone deacetylase inhibitors impair the elimination of HIV-infected cells by cytotoxic T-lymphocytes. PLoS Pathog 10:e1004287. https://doi.org/10.1371/journal.ppat.1004287.
13. Yang H-C, Xing S, Shan L, O'Connell K, Dinoso J, Shen A, Zhou Y, Shrum CK, Han Y, Liu JO, Zhang H, Margolick JB, Siliciano RF. 2009. Small-molecule screening using a human primary cell model of HIV latency

identifies compounds that reverse latency without cellular activation. J Clin Invest 119:3473–3486. https://doi.org/10.1172/JCI39199.
14. Ming C, Liu J, Duan P, Li M, Wen L. 2017. Biosynthesis and molecular engineering of templated natural products. National Sci Rev 4:533–575. https://doi.org/10.1093/nsr/nww045.
15. Kwok JM, Myatt SS, Marson CM, Coombes RC, Constantinidou D, Lam EW. 2008. Thiostrepton selectively targets breast cancer cells through inhibition of forkhead box M1 expression. Mol Cancer Ther 7:2022–2032. https://doi.org/10.1158/1535-7163.MCT-08-0188.
16. Qiao S, Lamore SD, Cabello CM, Lesson JL, Munoz-Rodriguez JL, Wondrak GT. 2012. Thiostrepton is an inducer of oxidative and proteotoxic stress that impairs viability of human melanoma cells but not primary melanocytes. Biochem Pharmacol 83:1229–1240. https://doi.org/10.1016/j.bcp.2012.01.027.
17. Bhat UG, Halasi M, Gartel AL. 2009. FoxM1 is a general target for proteasome inhibitors. PLoS One 4:e6593. https://doi.org/10.1371/journal.pone.0006593.
18. Bhat UG, Halasi M, Gartel AL. 2009. Thiazole antibiotics target FoxM1 and induce apoptosis in human cancer cells. PLoS One 4:e5592. https://doi.org/10.1371/journal.pone.0005592.
19. Sandu C, Ngounou Wetie AG, Darie CC, Steller H. 2014. Thiostrepton, a natural compound that triggers heat shock response and apoptosis in human cancer cells: a proteomics investigation. Adv Exp Med Biol 806:443–451. https://doi.org/10.1007/978-3-319-06068-2_21.
20. Pan XY, Zhao W, Wang CY, Lin J, Zeng XY, Ren RX, Wang K, Xun TR, Shai Y, Liu SW. 2016. Heat shock protein 90 facilitates latent HIV reactivation through maintaining the function of positive transcriptional elongation factor b (p-TEFb) under proteasome inhibition. J Biol Chem 291:26177–26187. https://doi.org/10.1074/jbc.M116.743906.
21. O'Keeffe B, Fong Y, Chen D, Zhou S, Zhou Q. 2000. Requirement for a kinase-specific chaperone pathway in the production of a Cdk9/cyclin T1 heterodimer responsible for P-TEFb-mediated Tat stimulation of HIV-1 transcription. J Biol Chem 275:279–287. https://doi.org/10.1074/jbc.275.1.279.
22. Kumar M, Rawat P, Khan SZ, Dhamija N, Chaudhary P, Ravi DS, Mitra D. 2011. Reciprocal regulation of human immunodeficiency virus-1 gene expression and replication by heat shock proteins 40 and 70. J Mol Biol 410:944–958. https://doi.org/10.1016/j.jmb.2011.04.005.
23. Anderson I, Low JS, Weston S, Weinberger M, Zhyvoloup A, Labokha AA, Corazza G, Kitson RA, Moody CJ, Marcello A, Fassati A. 2014. Heat shock protein 90 controls HIV-1 reactivation from latency. Proc Natl Acad Sci U S A 111:E1528–37. https://doi.org/10.1073/pnas.1320178111.
24. Kim M, Hosmane NN, Bullen CK, Capoferri A, Yang HC, Siliciano JD, Siliciano RF. 2014. A primary CD4(+) T cell model of HIV-1 latency established after activation through the T cell receptor and subsequent return to quiescence. Nat Protoc 9:2755–2770. https://doi.org/10.1038/nprot.2014.188.
25. Contreras X, Schweneker M, Chen CS, McCune JM, Deeks SG, Martin J, Peterlin BM. 2009. Suberoylanilide hydroxamic acid reactivates HIV from latently infected cells. J Biol Chem 284:6782–6789. https://doi.org/10.1074/jbc.M807898200.
26. Bullen CK, Laird GM, Durand CM, Siliciano JD, Siliciano RF. 2014. New ex vivo approaches distinguish effective and ineffective single agents for reversing HIV-1 latency in vivo. Nat Med 20:425–429. https://doi.org/10.1038/nm.3489.
27. Jordan A, Bisgrove D, Verdin E. 2003. HIV reproducibly establishes a latent infection after acute infection of T cells in vitro. EMBO J 22:1868–1877. https://doi.org/10.1093/emboj/cdg188.
28. Shan L, Deng K, Shroff NS, Durand CM, Rabi SA, Yang HC, Zhang H, Margolick JB, Blankson JN, Siliciano RF. 2012. Stimulation of HIV-1-specific cytolytic T lymphocytes facilitates elimination of latent viral reservoir after virus reactivation. Immunity 36:491–501. https://doi.org/10.1016/j.immuni.2012.01.014.
29. Wang S, Zheng Q, Wang J, Zhao Z, Li Q, Yu Y, Wang R, Liu W. 2015. Target-oriented design and biosynthesis of thiostrepton-derived thiopeptide antibiotics with improved pharmaceutical properties. Org Chem Front 2:106–109. https://doi.org/10.1039/C4QO00288A.
30. Duan P, Zheng Q, Lin Z, Wang S, Chen D, Liu W. 2016. Molecular engineering of thiostrepton: via single "base"-based mutagenesis to generate side ring-derived variants. Org Chem Front 3:1254–1258. https://doi.org/10.1039/C6QO00320F.
31. Wang J, Lin Z, Bai X, Tao J, Liu W. 2019. Optimal design of thiostrepton-derived thiopeptide antibiotics and their potential application against oral pathogens. Org Chem Front 6:1194–1199. https://doi.org/10.1039/C9QO00219G.
32. Laird GM, Bullen CK, Rosenbloom DI, Martin AR, Hill AL, Durand CM, Siliciano JD, Siliciano RF. 2015. Ex vivo analysis identifies effective HIV-1 latency-reversing drug combinations. J Clin Invest 125:1901–1912. https://doi.org/10.1172/JCI80142.
33. Abner E, Jordan A. 2019. HIV "shock and kill" therapy: in need of revision. Antiviral Res 166:19–34. https://doi.org/10.1016/j.antiviral.2019.03.008.
34. Harms JM, Wilson DN, Schluenzen F, Connell SR, Stachelhaus T, Zaborowska Z, Spahn CMT, Fucini P. 2008. Translational regulation via L11: molecular switches on the ribosome turned on and off by thiostrepton and micrococcin. Mol Cell 30:26–38. https://doi.org/10.1016/j.molcel.2008.01.009.
35. Du ZX, Zhang HY, Meng X, Gao YY, Zou RL, Liu BQ, Guan Y, Wang HQ. 2009. Proteasome inhibitor MG132 induces BAG3 expression through activation of heat shock factor 1. J Cell Physiol 218:631–637. https://doi.org/10.1002/jcp.21634.
36. Chaudhary P, Khan SZ, Rawat P, Augustine T, Raynes DA, Guerriero V, Mitra D. 2016. HSP70 binding protein 1 (HspBP1) suppresses HIV-1 replication by inhibiting NF-kappaB mediated activation of viral gene expression. Nucleic Acids Res 44:1613–1629. https://doi.org/10.1093/nar/gkv1151.
37. Vallabhapurapu S, Karin M. 2009. Regulation and function of NF-kappaB transcription factors in the immune system. Annu Rev Immunol 27:693–733. https://doi.org/10.1146/annurev.immunol.021908.132641.
38. Archin NM, Liberty AL, Kashuba AD, Choudhary SK, Kuruc JD, Crooks AM, Parker DC, Anderson EM, Kearney MF, Strain MC, Richman DD, Hudgens MG, Bosch RJ, Coffin JM, Eron JJ, Hazuda DJ, Margolis DM. 2012. Administration of vorinostat disrupts HIV-1 latency in patients on antiretroviral therapy. Nature 487:482–485. https://doi.org/10.1038/nature11286.
39. Manasanch EE, Orlowski RZ. 2017. Proteasome inhibitors in cancer therapy. Nat Rev Clin Oncol 14:417–433. https://doi.org/10.1038/nrclinonc.2016.206.
40. Zheng Q, Wang Q, Wang S, Wu J, Gao Q, Liu W. 2015. Thiopeptide antibiotics exhibit a dual mode of action against intracellular pathogens by affecting both host and microbe. Chem Biol 22:1002–1007. https://doi.org/10.1016/j.chembiol.2015.06.019.
41. Heimberger T, Andrulis M, Riedel S, Stuhmer T, Schraud H, Beilhack A, Bumm T, Bogen B, Einsele H, Bargou RC, Chatterjee M. 2013. The heat shock transcription factor 1 as a potential new therapeutic target in multiple myeloma. Br J Haematol 160:465–476. https://doi.org/10.1111/bjh.12164.
42. Rawat P, Mitra D. 2011. Cellular heat shock factor 1 positively regulates human immunodeficiency virus-1 gene expression and replication by two distinct pathways. Nucleic Acids Res 39:5879–5892. https://doi.org/10.1093/nar/gkr198.
43. Ammirante M, Rosati A, Gentilella A, Festa M, Petrella A, Marzullo L, Pascale M, Belisario MA, Leone A, Turco MC. 2008. The activity of hsp90 alpha promoter is regulated by NF-kappa B transcription factors. Oncogene 27:1175–1178. https://doi.org/10.1038/sj.onc.1210716.
44. Shan L, Rabi SA, Laird GM, Eisele EE, Zhang H, Margolick JB, Siliciano RF. 2013. A novel PCR assay for quantification of HIV-1 RNA. J Virol 87:6521–6525. https://doi.org/10.1128/JVI.00006-13.
45. Kim D, Langmead B, Salzberg SL. 2015. HISAT: a fast spliced aligner with low memory requirements. Nat Methods 12:357–360. https://doi.org/10.1038/nmeth.3317.
46. Rousseaux MW, Revelli J-P, Vázquez-Vélez GE, Kim J-Y, Craigen E, Gonzales K, Beckinghausen J, Zoghbi HY, 2018. Depleting Trim28 in adult mice is well tolerated and reduces levels of alpha-synuclein and tau. Elife 7:e36768 https://doi.org/10.7554/eLife.36768.
47. Zufferey R, Nagy D, Mandel RJ, Naldini L, Trono D. 1997. Multiply attenuated lentiviral vector achieves efficient gene delivery in vivo. Nat Biotechnol 15:871–875. https://doi.org/10.1038/nbt0997-871.
48. Bolger AM, Lohse M, Usadel B. 2014. Trimmomatic: a flexible trimmer for Illumina sequence data. Bioinformatics 30:2114–2120. https://doi.org/10.1093/bioinformatics/btu170.